Journal of Magnetism and Magnetic Materials 322 (2010) 1296–1299

Contents lists available at ScienceDirect

Journal of Magnetism and Magnetic Materials

journal homepage: www.elsevier.com/locate/jmmm

Magnetic properties of 3d transition metal chains on vicinal Cu(1 1 1) surface

H. Hashemi [a,*], W. Hergert [a], V.S. Stepanyuk [b]

[a] Fachbereich Physik, Martin-Luther-Universität Halle-Wittenberg, Friedemann-Bach-Platz 6, D-06099 Halle, Germany
[b] Max-Planck-Institut für Mikrostrukturphysik, Weinberg 2, D-06120 Halle/Saale, Germany

ARTICLE INFO

Available online 3 May 2009

Keywords:
Nanostructure
Magnetism
Electronic structure

ABSTRACT

Density functional theory (DFT) is applied in our study to describe magnetic properties of 3d transition metal (TM) nanowires on a stepped Cu(1 1 1) surface. The basic template to study such metallic chains on the Cu(1 1 1) surface is an embedded Fe chain at one-atom distance away from the upper edge of the monoatomic surface step. Chains of 3d transition metal atoms from Sc to Ni are added on top of the Fe chain. At the beginning of the 3d row, the chains show antiferromagnetic order. A small energy difference between ferromagnetic and antiferromagnetic order is obtained for the Mn–Fe system. Cr forms an antiferromagnetic chain, whereas Fe, Co, and Ni chains are ferromagnetically coupled to the embedded Fe chain.

1. Introduction

Dimensionality is one of the most important factors to tailor the properties of magnetic systems. One-dimensional (1D) electron systems [1] show unusual physical properties which has made the fabrication of such 1D systems a challenge of modern nanoscience. Nanowires are one of the most important objects of nanotechnology. The ultimate nanowire is a system of atoms essentially one atom wide and of a length which is large compared to the interatomic distance (high aspect ratio). It is experimentally extremely difficult to produce such systems, because it is hard to confine a single row of atoms and keep it in a straight line. A stepped substrate is the most common template to create 1D nanostructures. The progress achieved in the fabrication of artificial nanostructures has enabled the preparation of extended ultrathin nanowires which are uniform in thickness and perfect at the atomic scale. The main idea is to exploit the 1D symmetry provided by an array of parallel steps on a vicinal surface along which the deposited material can nucleate, a procedure called step decoration. Nanowires or nanostripes usually grow on lower terraces along an ascending step edge. The Cu(1 1 1) surface can be prepared with lots of atom-high steps (cf. Fig. 1(a)). Surprisingly, the observations of Shen et al. [2,3] have demonstrated that Fe nanostripes grow on the upper terrace of such a system.

An important investigation of Fe nanowire growth on a stepped Cu(1 1 1) surface was made by Mo et al. [4], who used total-energy calculations within the framework of density functional theory and showed that the growth of Fe nanowires is a two-stage process. Initially, Fe adatoms form an atomic row embedded into the Cu substrate behind a row of Cu atoms at the descending step (cf. Fig. 1(b)). During this process a very stable embedded 1D Fe structure is formed. In a following step, the embedded Fe row acts as an attractor for the Fe atoms deposited on the surface. Therefore, a secondary row of Fe atoms is formed on top of the embedded Fe chain (cf. Fig. 1(c)), because Fe–Fe bonds are stronger than Fe–Cu bonds. As a result, a very stable, one-atom-wide iron nanowire is formed on the Cu surface, involving this double-chain of Fe atoms, one chain buried in the surface behind a step, the second chain on top of the first. Subsequently, in a scanning tunneling microscopy (STM) investigation aided by density functional theory (DFT) calculations, Guo et al. [5] confirmed this growth process. In a recent study kinetic Monte Carlo (kMC) simulations elucidated the self-organization of Fe adatoms into a several atoms wide stripe on the stepped Cu(1 1 1) surface with such an embedded Fe chain as nucleation center of the growth process and attributed it to the Cu surface state mediated long-range Fe–Fe interactions [6].

Furthermore, the Cu(1 1 1) stepped surface with the embedded Fe chain could be used as an exemplary template for the deposition of other 3d transition metals to form wires on top of the Fe chain. It is the interplay between dimensionality, local environment, and magnetic properties which cause the special interest in such systems.

The interest in such 1D structures is also related to other experimental and theoretical studies. One-dimensional metal systems have been investigated on metal surfaces [7,8] but also on insulating surfaces [9,10]. *Ab initio* electronic structure methods are used to study isolated 3d transition metal (TM) atomic chains [11,12]. Mokrousov et al. [13] investigated free

* Corresponding author.
E-mail address: Hossein.Hashemi@physik.uni-halle.de (H. Hashemi).

0304-8853/$ - see front matter © 2009 Elsevier B.V. All rights reserved.
doi:10.1016/j.jmmm.2009.04.048

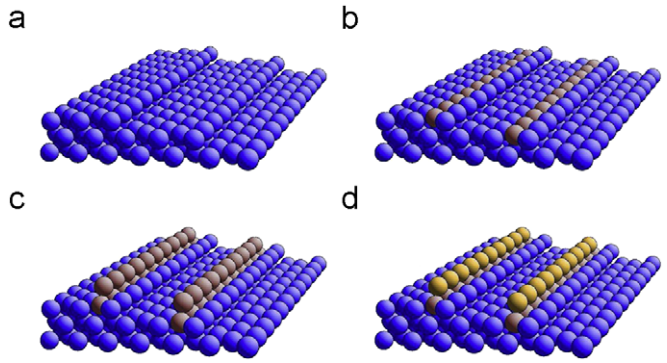

Fig. 1. Growth of TM–Fe double chains on Cu(1 1 1): (a) Clean Cu(1 1 1) stepped surface. (b) Deposition of Fe atoms (brown) on a stepped Cu (blue) surface. The Fe chain is embedded in the step behind a row of Cu atoms. (c) One-atom-wide Fe nanowire (brown) is formed, one chain of Fe embedded in the surface behind the step, the second Fe chain is formed on top of the first. (d) One-atom-wide TM nanowire (yellow) is formed on top of the embedded Fe chain. (For interpretation of the reference to color in this figure legend, the reader is referred to the web version of this article.)

standing 3d TM chains and such chains on (1 1 0) surfaces of Cu, Pd, Ag, and NiAl, while Spišák and Hafner [14] calculated electronic and magnetic properties of Fe nanowires at the step edge of vicinal Cu surfaces. Pick et al. [15] used a combination of *ab initio* and semi-empirical methods to calculate the magnetic anisotropy energy for Co chains on a stepped Cu(1 1 1) surface.

The purpose of the present work in contrast to other theoretical investigations, is to investigate, by means of *ab initio* electronic structure calculations, the magnetic structure of 3d TM chains which could be grown eventually by using the above mentioned template of a Cu(1 1 1) surface with an embedded Fe chain. (cf. Fig. 1(d)). Our study is focused on 3d TM elements, because they offer a wide scope of complex magnetic structures in higher dimensions and contain the bulk ferromagnets.

2. Computational details

In the first principles calculations reported here, the accurate frozen-core full-potential projector augmented-wave (PAW) method [16] is used as implemented in the VASP code [17,18] applying the Perdew–Wang 1991 version of the generalized gradient approximation (PW91-GGA). [19] The default values of the cutoff energy for the different elements are used. The Methfessel–Paxton approach [20] is employed to smear the electronic states near the Fermi level. A first-order approximation to the smearing function and a Gaussian width of 0.2 eV has been determined as the optimal choice. The total energy of the bulk fcc Cu was calculated to obtain the bulk lattice constants which is $a = 3.633$ Å, in good comparison with the experimental value of 3.615 Å [21]. To model the Cu(1 1 1) stepped surface, a supercell was constructed by stacking six layers including 60 Cu atoms, which was in turn rotated by a slab miscut along the [3 2 2] direction. At the end it consists of (1 1 1) terraces of five lateral lattice constants width separated by type A steps of monatomic height. The surface of the substrate constructed in this way and used in our calculation is depicted in Fig. 1(a). The distance from one slab to its nearest image is equivalent to 13.5 Å. The two-dimensional Brillouin zone is sampled using 33 k points.

The aim of our investigation is to compare the properties of free TM–Fe double chains with the same double chains embedded in the Cu(1 1 1) surface. The relaxations of free chains and the embedded chains are different. Preliminary results indicate that the whole scenario remains unchanged when lattice relaxation is allowed. Thus, structural relaxations are not taken into account. Both, the free double chains and the double chains embedded in the Cu(1 1 1) surface have interatomic distances in correspondence to the underlying Cu structure. This restriction allows to concentrate on the systematic changes in the magnetic structure by changing the kind of atom in the added chain through the 3d TM series.

3. 3d TM and Fe double free-standing chain

Due to symmetry five different magnetic configurations of the system consisting of one TM and one Fe chain are considered. The configurations are depicted in Fig. 2.

Now, the magnetic properties of free-standing double chains including Fe and TM chains with an interatomic distance corresponding to the Cu bond length have been investigated first. The total energy calculations, summarized in Table 1, reveal magnetic solutions for all the double chains. Not all magnetic configurations could be stabilized in the self-consistent electronic structure calculations. Furthermore, one can see that the Mn, Fe, Co, and Ni chains are most stable in the FM state, having a ferromagnetic coupling to the Fe chain, whereas the ground state of the Sc, Ti, and V chains is the AFM state characterized by the antiferromagnetic coupling of the TM chain to the Fe chain. The ground state configuration of Cr chains is of the M (mixed) type

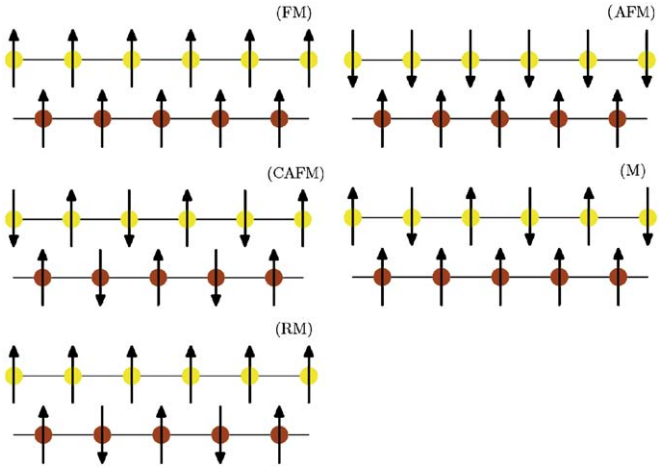

Fig. 2. Schematic view of possible magnetic configurations of a double chain consisting of TM (yellow) and Fe (brown) atoms: (FM) ferromagnetic coupling of Fe and TM chain, (AFM) the intra-chain coupling is ferromagnetic but the two chains are coupled antiferromagnetically, (CAFM) antiferromagnetic coupling in both chains, (M) mixed type, i.e. antiferromagnetic coupling in the TM chain and ferromagnetic coupling in Fe chain, (RM) reverse mixed, i.e. ferromagnetic coupling in TM chain but antiferromagnetic coupled Fe chain. (For interpretation of the reference to color in this figure legend, the reader is referred to the web version of this article.)

Table 1
Energy differences (meV/cell) for the different magnetic configurations (cf. Fig. 2) with respect to the ferromagnetic state for the free-standing double chains, consisting of a 3d transition metal chain and a Fe chain.

Configuration	Sc	Ti	V	Cr	Mn	Fe	Co	Ni
E_{AFM} (meV/cell)	−1153	−694	−710	−371	743	1225	1026	993
E_{M} (meV/cell)			−371	−600	161	837	716	
E_{RM} (meV/cell)	−670	−97	−82	195	645	837	752	520
E_{CAFM} (meV/cell)			−170	−364	478	1134	1165	

Table 2
Absolute values of magnetic moments in ground state configurations of free-standing TM–Fe double chains.

TM elements	Sc	Ti	V	Cr	Mn	Fe	Co	Ni
TM magnetic moment (μ_B)	0.70	1.56	2.61	3.53	4.07	3.05	2.04	0.88
Fe magnetic moment (μ_B)	2.69	2.77	2.85	2.97	2.90	3.05	3.14	3.17

Table 3
Energy differences (meV/cell) for the different magnetic configurations (cf. Fig. 2) with respect to the ferromagnetic state for the embedded double chains, consisting of a 3d transition metal chain and a Fe chain.

Configuration	Sc	Ti	V	Cr	Mn	Fe	Co	Ni
E_{AFM} (meV/cell)	−304	−205	−444	−350	412	732	473	387
E_{M} (meV/cell)			−163	−629	13	813	418	
E_{RM} (meV/cell)	151	461	153	149	650	721	652	507
E_{CAFM} (meV/cell)			186	−204	378	969	825	

(cf. Fig. 2). In this configuration the TM chain is antiferromagnetic by itself.

Table 2 contains the magnetic moments of the free-standing TM–Fe chains. The Fe chain moment increases slightly from Sc to Ni and is enhanced with respect to the bulk value due to the reduced number of neighbors. The variation of the moments in the TM chain follows the usual trend known from the free atoms and other 3d TM nanostructures (cf. [22]) Mn shows a high local moment as it was also obtained for Mn clusters on the Ag(1 0 0) surface [23].

4. 3d TM chains on the surface

In the following the influence of embedding of the TM–Fe wire into the Cu(1 1 1) surface (cf. Fig. 1(d)) is investigated. The change in the local environment and therefore the hybridization with the electronic states of the Cu substrate leads to the observed changes in the magnetic properties. Due to the embedding the atoms in the TM chain gain two additional Cu nearest neighbors to the two Fe nearest neighbors in the free-standing wire. The embedded Fe atoms have beside the two TM nearest neighbors additional seven Cu nearest neighbor atoms.

The ground state magnetic properties of TM chains deposited on the embedded Fe chain are summarized in Table 3. The energy difference is shown with respect to the ferromagnetic solution, i.e. a positive ΔE indicates a ferromagnetic ground state. Table 3 presents that the Mn, Fe, Co, and Ni chains are most stable in the FM state, while the ground state of the Sc, Ti, and V chains is the AFM state (cf. Fig. 2). Interestingly, the ground state for the Cr–Fe wire is from M-type. Using Cr to form the TM chain on the embedded Fe chain, the formation of a well-ordered antiferromagnetic Cr–Fe wire can be achieved.

The magnetic moments in the embedded configuration are smaller than in the corresponding freestanding double-chain (cf. 4). It can be seen that the change of the Fe moments in general is larger than the change of the TM moments due to the stronger hybridization effects. This can be seen clearly for the Fe–Fe wire. The substrate brakes the symmetry and the embedded chain has a strongly reduced moment while the moment of the chain on the surface is unchanged.

Note, the Mn chain exhibits a bistability between the FM and M states ($\Delta E < 13$ meV/supercell). This energy difference is smaller than the energy differences between magnetic states which have been calculated for Mn clusters on Ag(0 0 1) [23]. Such small energy differences open up the possibility to influence the magnetic state by external means at finite temperature. It should be noted that the energy difference will depend on structural relaxations at the surface which are not taken into account in the present investigation.

Table 4
Absolute values of magnetic moments in ground state configurations of the embedded TM–Fe double chains.

TM elements	Sc	Ti	V	Cr	Mn	Fe	Co	Ni
|TM magnetic moment| (μ_B)	0.25	1.04	2.54	3.56	3.90	3.09	2.02	0.84
|Fe magnetic moment| (μ_B)	2.19	2.29	2.41	2.55	2.54	2.62	2.71	2.76

The systematic investigation of different magnetic states can be used as a starting point to consider the finite temperature magnetic properties of arrays of such TM–Fe wires. If the magnetic states are mapped onto a classical Heisenberg model, the Heisenberg exchange parameters can be determined from the energy differences given in Table 3. Preliminary calculations indicate that Monte Carlo simulations can be used to determine the magnetic properties at finite temperature.

In summary, we have performed first-principles calculations of magnetic states in TM–Fe double-chains on the vicinal Cu surface, whereas Fe forms a buried row in the Cu(1 1 1) surface and a transition metal chain is positioned at the top of the Fe wire. A transition from antiferromagnetic (AFM, M) to ferromagnetic (F) configurations between Fe and TM is found in the middle of the 3d series. In the Cr–Fe system the Cr chain is ordered antiferromagnetically. In all the other configurations the TM chains are intrinsically in ferromagnetic order. The stepped surface with embedded Fe chain can be used to form 1D magnetic systems with very different magnetic properties experimentally .

Acknowledgments

We thank N.N. Negulyaev and P.A. Ignatiev for fruitful discussions. The work was supported by the cluster of excellence "Nanostructured Materials" of the state Saxony-Anhalt and the International Max Planck Research School for Science and Technology of Nanostructures.

References

[1] P. Segovia, D. Purdie, M. Hengsberger, Y. Baer, Nature (London) 402 (1999) 504.
[2] J. Shen, R. Skomski, M. Klaua, H. Jenniches, S.S. Manoharan, J. Kirschner, Phys. Rev. B 56 (1997) 2340.
[3] J. Shen, M. Klaua, P. Ohresser, H. Jenniches, J. Barthel, C.V. Mohan, J. Kirschner, Phys. Rev. B 56 (1997) 11134.
[4] Y. Mo, K. Varga, E. Kaxiras, Z. Zhang, Phys. Rev. Lett. 94 (2005) 155503.
[5] J. Guo, Y. Mo, E. Kaxiras, Z. Zhang, H.H. Weitering, Phys. Rev. B 73 (2006) 193405.
[6] H.F. Ding, V.S. Stepanyuk, P.A. Ignatiev, N.N. Negulyaev, L. Niebergall, M. Wasniowska, C.L. Gao, P. Bruno, J. Kirschner, Phys. Rev. B 76 (2007) 033409.
[7] P. Gambardella, A. Dallmeyer, K. Maiti, M.C. Malagoli, W. Eberhardt, K. Kern, C. Carbone, Nature 416 (2002) 301, 4 pages.
[8] H. Fujisawa, S. Shiraki, M. Furakawa, S. Ito, T. Nakamura, T. Muro, M. Nantoh, M. Kawai, Phys. Rev. B 75 (2007) 245423 p. 8.
[9] C.F. Hirjibehedin, C.P. Lutz, A.J. Heinrich, Science 312 (2006) 1021.
[10] C. Tegenkamp, J. Phys. Condens. Matter 21 (2009) 013002, (18 pages).
[11] J.C. Tung, G.Y. Guo, Phys. Rev. B 76 (2007) 094413.
[12] C. Ataca, S. Cahangirov, E. Durgun, Y.-R. Jang, S. Ciraci, Phys. Rev. B 77 (2008) 214413, (12 pages).
[13] Y. Mokrousov, G. Bihlmayer, S. Blügel, S. Heinze, Phys. Rev. B 75 (2007) 104413.
[14] D. Spišák, J. Hafner, Phys. Rev. B 65 (2002) 235405.
[15] Š. Pick, P.A. Ignaiev, A.L. Klavsyuk, W. Hergert, V.S. Stepanyuk, P. Bruno, J. Phys. Condens. Matter 19 (2007) 446001, (11 pages).
[16] P.E. Blöchl, Phys. Rev. B 50 (1994) 17953.
[17] G. Kresse, J. Hafner, Phys. Rev. B 48 (1993) 13115.

[18] G. Kresse, J. Furthmüller, Phys. Rev. B 54 (1996) 11169.
[19] J.P. Perdew, Y. Wang, Phys. Rev. B 45 (1992) 13244.
[20] M. Methfessel, A.T. Paxton, Phys. Rev. B 40 (1989) 3616.
[21] M.E. Straumanis, L.S. Yu, Acta Crystallogr. Sect. A 25 (1969) 676–682.
[22] V.S. Stepanyuk, W. Hergert, P. Rennert, K. Wildberger, R. Zeller, P.H. Dederichs, Surf. Sci. 377–379 (1997) 495.
[23] V.S. Stepanyuk, W. Hergert, K. Wildberger, S.K. Nayak, P. Jena, Surf. Sci. 384 (1997) L892.